Improvement of PET surface modification using APPJ with different shielding gases

Mehrnoush Narimisa[1], Iuliia Onyshchenko[1], Rino Morent[1], Nathalie De Geyter[1]

[1]*Research Unit Plasma Technology (RUPT), Department of Applied Physics, Faculty of Engineering and Architecture, Ghent University, Ghent, Belgium*

Abstract: This work demonstrates the enhancement in polyethylene terephthalate (PET) surface treatment by an atmospheric pressure plasma jet (APPJ) with a modified design. The influence of different shielding gas introduction on the plasma surface treatment potential is studied. Optical emission spectroscopy (OES) is carried out to visualize differences in discharge composition for various APPJ set-ups. These results are compared with changes in PET surface wettability and chemical composition.

Keywords: plasma treatment, atmospheric pressure plasma jet, PET, shielding gas

1. Introduction

Atmospheric pressure plasmas have a lot of advantages in comparison to medium or low-pressure plasmas, such as simple construction, rich plasma chemistry, no need for expensive vacuum equipment, flexibility in scaling up for industrial level, etc. A stable and high rate of the publications dealing with APPJ in the last decade indicates a standing interest in this type of plasma source. Besides the already mentioned benefits of atmospheric pressure discharges, plasma jets can also be used for surface treatment of 3D structures and samples with complex geometries [1]. The range of APPJ applications is huge and covers many research fields like physics, chemistry, materials, biochemistry, medicine, etc. [2-3]. Regardless of the already tremendous interest in using plasma jets for various needs, the research never stops since a lot of newer areas also demand this plasma source for their needs [4-5]. However, the requirements to the APPJ vary for each specific application, as such, there is a need in creating new plasma jets or modifying already existing sources. Nonetheless, enhancing the effectiveness of these sources has remained challenging. There are a few works that deal with the improvement of APPJ treatment efficiency which for example modify the geometry of the APPJ set-up [6-7], change plasma gas composition [8], control ambient conditions [9] or make some external adjustments [10]. This particular work is focused on modifying an existing APPJ design to precisely control the ambient conditions around a typical plasma jet [11]. First of all, the composition of the redesigned discharge will be examined by using OES. The influence of the plasma source geometry and the ambient gas on the plasma plume composition will also be demonstrated. Hereafter, the surface treatment of polyethylene terephthalate (PET) will be performed with different experimental conditions. The degree of plasma impact on the polymer surface will be determined using water contact angle (WCA) measurements and X-ray photoelectron spectroscopy (XPS) analysis. The changes in surface wettability and chemical composition will be correlated with APPJ design and treatment conditions.

2. Experimental part

The plasma source used in this work is a modification of the APPJ reported by Onyshchenko et. al. [10-11]. The change to the original set-up includes an introduction of a shielding gas to the gap between the sample and the edge of the plasma jet capillary. Three holes at 10 mm radial distance from the centre of the capillary are drilled in a polyvinyl chloride (PVC) disc at 45° with respect to the vertical axis and towards the plasma plume. Tubes with 3 mm inner diameter and 4 mm outer diameter are fit in the holes on one side and connected to a mass flow controller on the other side. The geometry of experimental setup has mirror symmetry axis due to the location of inlets for shield gases. All the measurements in this work are performed along the symmetry axis (see fig.1) since it presents all possible variations in the system.

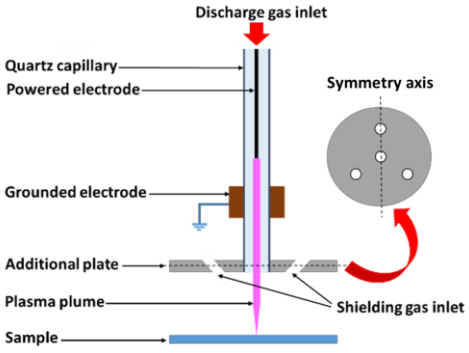

Fig. 1. Schematic representation of the experimental plasma jet with top view of an additional plate with holes.

Fig. 1 shows the schematic representation of the experimental set-up used in this work. The plasma jet is ignited in argon (Air Liquide, Alphagaz 1) gas that is

flowing through the capillary at a flow rate of 1 standard litre per minute (slm) after applying a high voltage between the powered and grounded electrodes. A power supply produces an AC high voltage signal with a fixed frequency of 60 kHz and fixed amplitude of 8 kV (peak-to-peak). A high voltage probe (Tektonix P6015A) and a current transformer (Pearson Current Monitor Model 2877) are connected to a Picoscope 3204A digital oscilloscope to record voltage-current waveforms. The average discharge power has been calculated using the following equation:

$$W = \frac{1}{T}\int_{t}^{t+T} I(t)V(t)dt \qquad (1)$$

where integration is averaged over one period (T). Nitrogen (Air Liquide, Alphagaz 1) or argon is used as shielding gas with 1 slm flow rate through each of the three tubes. Squared PET samples (65×65 mm^2) purchased from Goodfellow, Germany, with 250 µm thickness have been used without any pre-treatment as substrates. The samples are placed 10 mm underneath the end of the capillary and exposed to the plasma during 10 s for all experiments in this work.

Space-resolved optical emission spectroscopy (OES) 1.4 nm along the vertical symmetry axis of the APPJ set-up. The resultant spectra in this work are presented as arbitrary units of intensity.

One of the essential surface parameters is its wettability. Static water contact angle (WCA) measurements are carried out using a commercial Easy Drop optical system (Krüss GmbH, Germany) to determine the changes in surface wettability after plasma treatment using different experimental conditions. The measurements are performed in ambient air at room temperature immediately after the plasma exposure. Small droplets (1 µl) of distilled water are placed along the symmetry axis on the sample. Computer software, provided with the instrument, automatically defines the value of contact angle from the image of the water droplet on the surface, recorded with a CCD video camera. In this work, Laplace-Young curve fitting is used to determine the WCA values which have an estimated error of less than 2.0° with 95% probability for each conducted measurement.

The changes in chemical composition after the plasma treatments are defined by X-ray photoelectron spectroscopy (XPS). A PHI Versaprobe II spectrometer is used to record survey and detailed C1s spectra of plasma treated samples along the symmetry axis with 2 mm distance between each measurement point. This machine is equipped with a monochromatic Al K_α X-ray source (hν = 1486.6 eV) operated at 25 W. Wide range and narrow scans are recorded in a vacuum of at least 10^{-6} Pa with a pass energy of 187.85 and 23.5 eV respectively at a take-off angle of 45° relative to the sample surface. The elemental composition and the chemical shifts in C1s peaks are determined from survey and detailed C1s spectra respectively using Multipak software (v 9.6). The energy scale is calibrated with respect to the hydrocarbon component of the C1s spectrum (285.0 eV) and the deconvolution is performed by utilizing Gaussian−Lorentzian peak shapes with the full-width at half maximum (FWHM) of each line shape set to less than 1.5 eV.

3. Results and discussion

In the first step, measurements of applied voltage and discharge current have been conducted to characterize the electrical behaviour of the plasma. Subsequently, the average power (W) is determined based on discharge-current waveforms using equation (1). The calculated power values are listed in Table 1. The obtained values do not change significantly and stays below 4.3W. However, small variations are observed due to the changes in the set-up geometry or in the ambient conditions. As can be noticed, the highest power is obtained for the typical plasma jet where no modifications to the set-up are done. However, an additional plate from a recent APPJ design [10] decreases the value of discharge power the most (0.26 W) since in this case the PVC plate behaves as another capacitor. Consequently, the total capacitance of the set-up (plasma jet capillary and additional plastic plate) will be smaller than before modification and thus the total power will decrease as well. However, when the sample is placed 10 mm below the jet, the discharge power slightly increases due to limitation of the energy dissipation in ambient air. In contrast, introducing N_2 as a shield gas has negligible influence on the discharge power. In contrast, using Ar as shield gas enhances power of the discharge since it helps the plasma to propagate further and occupy more space.

Table 1. APPJ discharge power for different conditions.

Condition	Power (W)
Typical design	4.26 ± 0.04
New design	4.00 ± 0.05
With sample; no shield gas	4.11 ± 0.01
With sample; 3slm N_2 shield gas	4.12 ± 0.02
With sample; 3slm Ar shield gas	4.20 ± 0.08

To gather information on the type and amount of excited species, OES measurements are employed. Fig. 2.a presents the OES spectra obtained along the vertical axis of the plasma plume at 10 mm distance from the edge of the jet capillary. The results clearly show that the new adjustment to the plasma jet design causes a higher amount of reactive species production in comparison to the typical plasma jet set-up. This result can be explained by changes in the gas flow dynamics produced by the additional plate. However, it should be mentioned that no new lines or bands have been observed in these spectra suggesting that the additional plate has no influence on the type of plasma species. Moreover, the influence of the shield gas on the discharge composition is also investigated when the

sample is located at 10 mm away from the bottom of the capillary. A comparison of fig. 2b suggests that the intensity of recorded OES spectra of plasma jet with a new design significantly increases in the second case where Ar is used as shield gas which can be due to limited dissipation of excited states when there is less mixing with ambient air. As can be observed from fig. 2.b, introducing argon shield gas results in an increase in the amount of excited states. A possible explanation for this behaviour is as following: extra argon gas mixes with the plasma in the afterglow and confines the air access which extends the lifetime of argon excited states. This process does not exclude the possibility of energy transfer from excited argon to N_2. However, adding nitrogen shield gas slightly increases the N_2 excited states while strongly decreasing the argon reactive states. Indeed, nitrogen attenuates the process of producing excited N_2 species by making use of energy from Ar^* states.

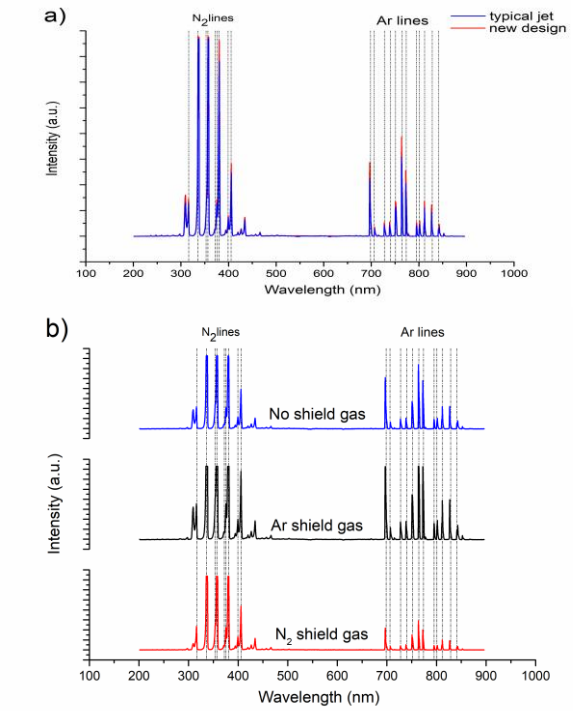

Fig. 2 a) Optical emission spectra obtained for typical APPJ and with a new design; b) OES results for APPJ with a new design without and with different shielding gases.

Wettability of the PET samples is also quantified with WCA measurements. For the untreated sample, the contact angle value is recorded to be 87°. Fig. 3 demonstrates the WCA profile along the symmetry axis without any shielding gas and with 1 slm argon and nitrogen shield gases through each of three additional tubes. It is observed that the minimum value in the centre of the sample is slightly higher when introducing argon shield gas. Also, the width of the hydrophilic region considerably increases under this condition. Moreover, the sample experiences the impact of shield gas on the sample edges as well. However, nitrogen shield gas does not improve the wettability of the PET samples significantly. These results are in good agreement with the OES data obtained before. In the case of Ar shielding gas, extra excited species are detected at this location in comparison to other conditions. Thus, only Ar is able to provide an extra treatment of the sample surface. It can be concluded that argon as shield gas can activate the surface and enhance the wettability of the sample at longer distances from the plasma jet centre.

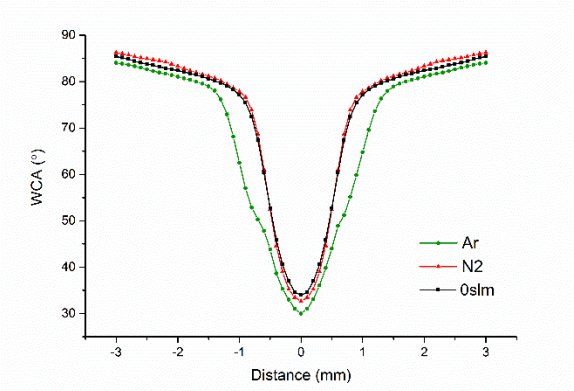

Fig. 3. Water contact angle distribution along the symmetry axis of a PET sample for different shield gas types.

In the next step, the atomic composition of the plasma treated PET samples is examined using low resolution XPS survey along the symmetry axis of the PET samples. For the untreated sample, the percentage of oxygen is measured to be 22%. Fig. 4 demonstrates the distribution of total oxygen content along the sample after plasma treatment using different shield gases. The first noticeable result is that Ar shield gas contributes to a higher incorporation of oxygen in the centre of the treated sample surface in comparison to the experiment without any additional gas. Furthermore, N_2 shielding gas does not reveal a significant increase in the width of the incorporated oxygen region as the width remains almost the same as for the treatment without any additional gas. The most significant changes are observed for the experimental condition in which Ar is used as shielding gas which is in good agreement with the obtained WCA results. To get more insight, deconvolutions of high resolution C1s peaks have also been performed. The fit is performed by combining three Gaussian−Lorentzian peak shapes at 285, 286.3 and 288.8 eV which correspond to C-C/C-H, C-O and O-C=O groups respectively [12]. Table 2 contains the results of the XPS high resolution C1s peak deconvolution for untreated and plasma treated samples with different conditions at 4 mm radial distance from the centre of the capillary. Based on these results, it can be concluded that no new bonds are detected on the PET surface after plasma treatment and thus, only the percentages of the different chemical groups present on the pristine PET sample have been changed. In detail, all performed plasma surface modifications increase the amount of all oxygen containing groups. However, as expected, in the case of argon shielding gas, the increase in

oxygen functionalities is the most pronounced. Adding N_2 shield gas does not have a great impact as the oxygen surface functionalities approximately remain the same as for the samples treated without any additional gas. These results are thus in good agreement with the earlier mentioned WCA and oxygen content results. Specifically, the wettability degree can be directly linked to the content of the oxygen containing polar groups which are responsible for hydrophilic characteristics of the surface of the sample [13-15]. Thus, it can be concluded that plasma treatment in general and with argon as shielding gas especially increases the percentage of the polar oxygen groups on the treated PET surface.

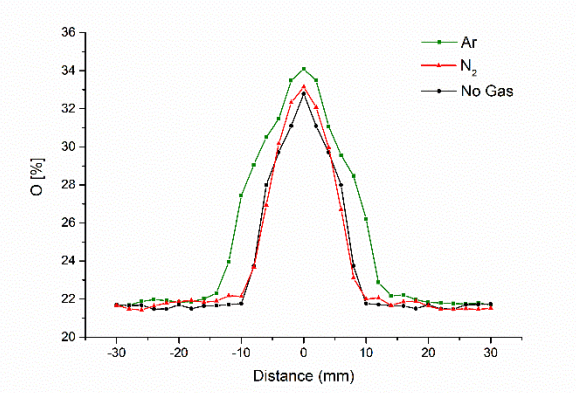

Fig. 4. Evolution of oxygen concentration on plasma treated PET surfaces along the symmetry axis for different shield gas types.

Table 2. Results of XPS high resolution C1s peak deconvolution for untreated and plasma treated PET samples at 4 mm distance from the sample centre.

Group	Untreated (%)	No shield gas (%)	N_2 (%)	Ar (%)
C-C/C-H	71.6 ± 1.8	61.3 ± 2.1	61.2 ± 1.0	58.1 ± 2.0
C-O	18.1 ± 1.5	23.7 ± 1.2	24.0 ± 0.8	26.7 ± 1.3
O-C=O	10.3 ± 1.6	15.0 ± 0.9	14.8 ± 0.4	15.1 ± 1.7

4. Conclusion

The main result of this work demonstrated the importance of ambient conditions during plasma jet treatment of polymer surfaces. First of all, the discharge power of the plasma jet changes depending on two factors: the whole system capacitance and the contact area with ambient air. The highest discharge power was observed for a typical design and the lowest for the modified plasma jet. Moreover, using Ar shield gas increased the discharge power. OES demonstrated that adding a plate at the edge of the plasma jet capillary results in a higher amount of excited states in the discharge. The intensity of the OES peaks suggested that different amounts of excited atoms and molecules were present in the plasma jet depending on the shielding gas type. The most noticeable change in the intensities was observed for the experimental conditions when argon was used as a shielding gas. Additionally, the same experimental condition improved the wettability area in comparison to all other used conditions in this work. Finally, XPS results revealed an increase in concentration of oxygen containing polar groups and overall oxygen concentration when adding argon shielding gas. All obtained results are in excellent agreement with each other. It was thus demonstrated that argon as a shielding gas has the biggest impact on surface properties after polymer treatment.

5. Acknowledgement

The research leading to these results has received funding from the Special Research Fund of Ghent University.

6. References

[1] I. Onyshchenko, N. De Geyter, A. Y. Nikiforov, and R. Morent, *Plasma Process. Polym.*, vol. 12, no. 3, pp. 271–284, 2015.

[2] J. K. Lee, M. S. Kim, J. H. Byun, K. T. Kim, G. C. Kim, and G. Y. Park, *Jpn. J. Appl. Phys.*, vol. 50, no. 8 PART 2, 2011.

[3] O. Guaitella and A. Sobota, *J. Phys. D. Appl. Phys.*, vol. 48, no. 25, p. 255202, 2015.

[4] S. Rupf *et al.*, *J. Med. Microbiol.*, vol. 59, no. 2, pp. 206–212, 2010.

[5] A. A. P. Microjet *et al.*, vol. 38, no. March, pp. 1892–1896, 2017.

[6] Q. Y. Nie, C. S. Ren, D. Z. Wang, and J. L. Zhang, *Appl. Phys. Lett.*, vol. 93, no. 1, pp. 17–20, 2008.

[7] A. H. R. Castro, K. G. Kostov, and V. Prysiazhnyi, *IEEE Trans. Plasma Sci.*, vol. 43, no. 9, pp. 3228–3233, 2015.

[8] A. F. H. Van Gessel, K. M. J. Alards, and P. J. Bruggeman, *J. Phys. D. Appl. Phys.*, vol. 46, no. 26, 2013.

[9] C. Y. Chou *et al.*, *RSC Adv.*, vol. 5, no. 57, pp. 45662–45667, 2015.

[10] I. Onyshchenko, N. De Geyter, and R. Morent, *Plasma Process. Polym.*, vol. 14, no. 8, 2017.

[11] I. Onyshchenko, A. Y. Nikiforov, N. De Geyter, and R. Morent, *Plasma Process. Polym.*, vol. 12, no. 5, pp. 466–476, 2015.

[12] C. B. Miller and P. A. Wheeler, vol. 20, p. 12172, 2014.

[13] K. Gotoh, Y. Kobayashi, A. Yasukawa, and Y. Ishigami, *Colloid Polym. Sci.*, vol. 290, no. 11, pp. 1005–1014, 2012.

[14] Q. T. Le, J. J. Pireaux, R. Caudano, and P. Leclere, no. May 2013, pp. 999–1023, 2012.

[15] C. Cheng, Z. Liye, and R. J. Zhan, *Surf. Coatings Technol.*, vol. 200, no. 24, pp. 6659–6665, 2006.